ACS Energy LETTERS

http://pubs.acs.org/journal/aelccp

Stable, Impermeable Hexacyanoferrate Anolyte for Nonaqueous Redox Flow Batteries

Yuyue Zhao,[†] Sambasiva R. Bheemireddy,[†] Diqing Yue, Zhou Yu, Mohammad Afsar Uddin, Haoyu Liu, Zhiguang Li, Xiaoting Fang, Xingyi Lyu, Garvit Agarwal, Zhangxing Shi, Lily A. Robertson, Lei Cheng, Tao Li, Rajeev S. Assary, Venkat Srinivasan, Susan J. Babinec, Zhengcheng Zhang, Jeffrey S. Moore, Ilya A. Shkrob,* Xiaoliang Wei,* and Lu Zhang*

Cite This: *ACS Energy Lett.* 2024, 9, 4273−4279

Read Online

ACCESS | Metrics & More | Article Recommendations | Supporting Information

ABSTRACT: **Redox-active molecules, or redoxmers, in nonaqueous redox flow batteries often suffer from membrane crossover and low electrochemical stability. Transforming inorganic polyionic redoxmers established for aqueous batteries into nonaqueous candidates is an attractive strategy to address these challenges. Here we demonstrate such tailoring for hexacyanoferrate (HCF) by pairing the anions with tetra-*n*-butylammonium cation (TBA^+). TBA_3HCF has good solubility in acetonitrile and >1 V lower redox potential vs the aqueous counterpart; thus, the familiar aqueous catholyte becomes a new nonaqueous anolyte. The lowering of redox potential correlates with replacement of water by acetonitrile in the solvation shell of HCF, which can be traced to H-bond formation between water and cyanide ligands. Symmetric flow cells indicate exceptional stability of HCF polyanions in nonaqueous electrolytes and Nafion membranes completely block HCF crossover in full cells. Ion pairing of metal complexes with organic counterions can be effective for developing promising redoxmers for nonaqueous flow batteries.**

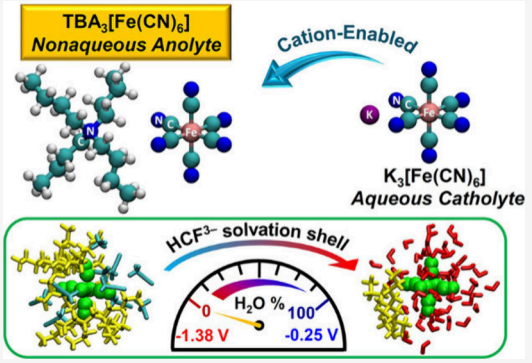

The intermittency of renewable power sources requires connection to energy storage systems to stabilize the output power and facilitate smooth integration to the power grid. Redox flow batteries (RFBs) are electrochemical storage devices that carry energy by redox-active materials (redoxmers) in liquid electrolytes.[1] Energy conversion occurs when the electrolytes are pumped through porous electrodes where the redoxmers are reversibly charged and discharged. This cell design enables decoupling of energy and power that are determined by electrolyte volume and cell stacking, respectively. Thus, RFBs have significant advantages of scalability, flexible design, modular manufacturing, active thermal management, and improved safety, making them highly promising for large-scale grid storage applications.[2,3] Significant progress and precommercial scale demonstrations have been achieved for aqueous RFBs over the past decades. However, the narrow elecrochemical window (<1.5 V), limited energy density, and expensive materials present major hurdles. In this regard, *nonaqueous* RFBs have several potential advantages over their *aqueous* counterparts.[4,5] The use of organic solvents widens the electrochemical window (>2 V) and expands the choice of redoxmers, suggesting a viable way of achieving the balance in their properties.

A variety of redox chemistries have been developed for nonaqueous RFBs, including organometallic,[6] organic,[7] and polymer[8] compounds. In some cases, the same redox core can be used in aqueous *and* nonaqueous environments, and successful examples include 2,2,6,6-tetramethylpiperidine-1-oxyl (TEMPO),[9,10] ferrocene,[11,12] viologen,[13,14] and phenazine.[15,16] Transition metal ions, such as vanadium, nickel, chromium, and iron, have been modified with organic ligands to produce soluble complexes for use in nonaqueous RFBs,[6] while other redoxmers (such as lithium iodide) are soluble in both types of electrolytes without modification.[17] However, it remains a challenge to combine good solubility and high stability in all states of charge, suitable redox potential, fast charge transfer kinetics, and low cost.[18−20] Therefore, new strategies are needed to simultaneously improve multiple properties.

Received: May 21, 2024
Revised: July 8, 2024
Accepted: July 23, 2024
Published: August 6, 2024

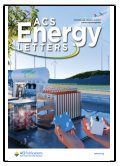

https://doi.org/10.1021/acsenergylett.4c01351
ACS Energy Lett. 2024, 9, 4273−4279

Scheme 1. Metathesis Synthesis of TBA_3HCF

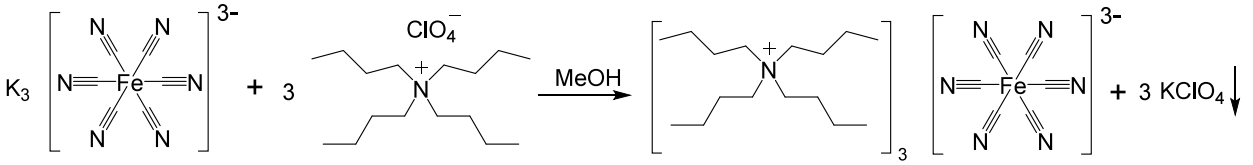

In this work, we report an effective strategy for transforming the well-studied aqueous hexacyanoferrate(II/III) redox couple ($HCF^{3-/4-}$) into a novel *nonaqueous* redoxmer by pairing this anion with the tetra-*n*-butylammonium cation (TBA^+). We show that this transformation bestows new properties on this polyanion that sharply differentiate it from the related aqueous system.

Aqueous potassium and sodium hexacyanoferrates (HCF) are well-established catholyte compounds with a redox potential of 0.40 V vs the standard hydrogen electrode (SHE). These redoxmers have been used in neutral and alkaline aqueous RFBs, where their slow aquation is a major parasitic reaction limiting their use in such devices.[21,22] The alkali salts of HCF are insoluble in aprotic solvents such as acetonitrile (MeCN). The TBA^+ cation has been known for its ability to solubilize the vanadium-containing Amavadin for energy-dense nonaqueous RFBs,[23] and we reasoned that pairing of TBA and HCF can yield a MeCN-soluble ionic compound. TBA_3HCF was synthesized via a facile one-step metathesis reaction between potassium hexacyanoferrate (III) and tetrabutylammonium perchlorate ($TBAClO_4$) in methanol with a yield of 84%, taking advantage of the negligible solubility of potassium perchlorate ($KClO_4$) in methanol (Scheme 1, Section S1, and Figures S1−S3). TBA_3HCF has a solubility of 0.59 M in neat MeCN, and 0.31 M in MeCN containing 1 M tetrabutylammonium hexafluorophospate ($TBAPF_6$), respectively. The 0.1−0.4 M solutions of TBA_3HCF in MeCN exhibit ionic conductivities over 10 mS cm^{-1} (Section S2, Figure S7) that are comparable to common supporting electrolytes for nonaqueous RFBs.[24] This feature can eliminate the need of costly supporting salt and simplify electrolyte composition.

To evaluate the electrochemical properties of TBA_3HCF, cyclic voltammetry (CV) was used to determine the redox potential and kinetics in nonaqueous electrolytes (Section S3). As shown in Figure 1a, the HCF anion has a low redox potential of −1.38 V vs Ag/Ag^+ in MeCN. Similarly low potentials were observed in propylene carbonate, *N*,*N*-dimethylformamide, and dimethyl sulfoxide (Figure S9), which is in agreement with previous studies.[25−27] These sharply negative potentials imply that in *nonaqueous* RFBs (unlike in their aqueous counterparts), the HCF polyanion is an *anolyte*: as such, it compares favorably with the best organic anolyte redoxmers.[28,29] Notably, adding water to MeCN shifts the redox potential to more positive values (Figure 1b). Throughout this composition change, the one-electron redox reaction remains fully reversible (Section S3). By using the Randles−Sevcik analysis (Figure S10a-b), the diffusion coefficient of HCF was estimated and used to characterize the redox kinetics using the Nicholson method (Figures S10c-d).[30] The electrochemical rate constant (k_0) of HCF is 6.53×10^{-3} cm s^{-1}, which is close to organic redoxmers.[28,29]

Molecular dynamics (MD) simulations (Section S5) were performed to understand the behaviors shown in Figure 1. Figure 2a shows a snapshot of the environment around HCF polyanion for 0.124 M TBA_3HCF in MeCN (Figure S15). On average, in this solution 9.2 MeCN molecules and stoichiometric 3 TBA^+ cations are coordinated with the anion. At this concentration, each TBA^+ cation contacts 16.6 solvent molecules, a single HCF^{3-} anion, and 1.93 other TBA^+ cations. The strong association between the ions seen in our MD calculations is also observed in small-angle X-ray

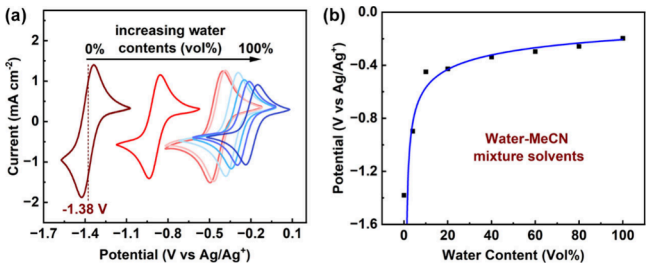

Figure 1. (a) Cyclic voltammograms for 10 mM TBA_3HCF in 0.5 M TBA^+ salt with a potential sweep rate of 100 mV s^{-1}. $TBAPF_6$ was used in 100 vol % MeCN and tetrabutylammonium chlroride (TBACl) was used in water-containing electrolytes due to the limited solubility of $TBAPF_6$ in water; the redox potentials were calibrated to the cases of $TBAPF_6$ according to Figure S8. (b) Redox potential as a function of water content (filled squares).

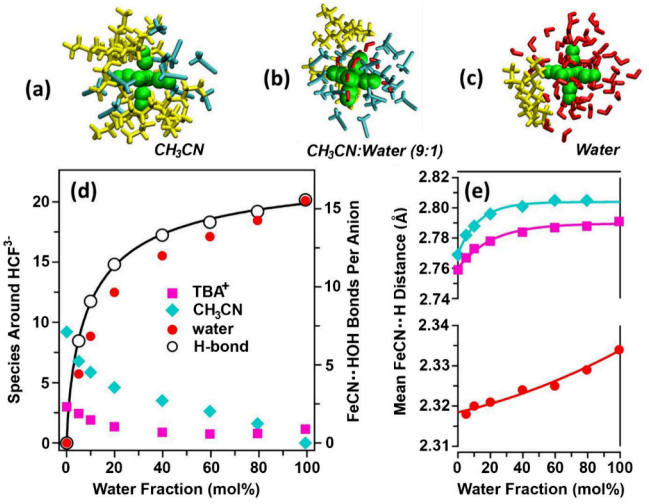

Figure 2. (a−c) Snapshots of HCF^{3-} (*green*) in solutions of TBA_3HCF (TBA^+ in *yellow*) in (a) MeCN (*cyan*), (b) 10 mol % (i.e., 4 vol %) water in MeCN, and (c) water (*red*). (d) *Left*: Composition of a solvation shell around HCF^{3-} plotted as a function of water mole fraction (see the color legend in the plot). *Right* (*open circles*): Number of FeCN···HOH hydrogen bonds per HCF^{3-} vs water mole fraction. (e) Average closest approach distances from HCF^{3-} nitrogen atoms to TBA^+ cations or solvent molecules vs water content. The color key for this plot is given in panel d.

https://doi.org/10.1021/acsenergylett.4c01351
ACS Energy Lett. 2024, 9, 4273−4279

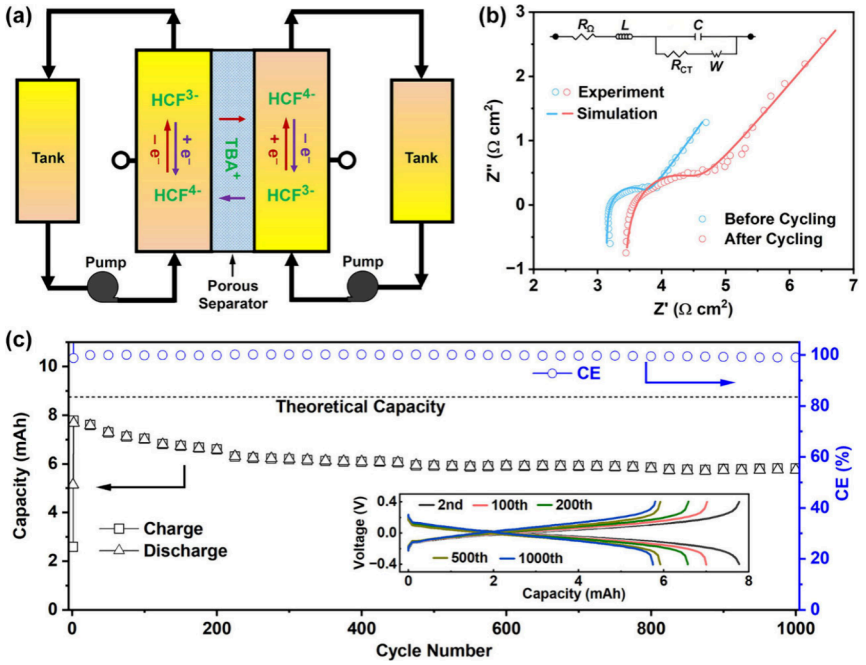

Figure 3. Symmetric flow cell test of $TBA_{3/4}HCF$: (a) schematic illustration of the cell setup; (b) experimental and simulated Nyquist plots before and after the cycling; (c) cycling capacity, CE, and voltage profiles (inset) over 1000 cycles. The electrolyte was 50 mM $TBA_{3/4}HCF$ in 1 M $TBAPF_6$ in MeCN. The current density was at 5 mA cm^{-2}, and the voltage cutoffs were −0.4 and 0.4 V.

scattering (SAXS) of TBA_3HCF solutions, where a correlation peak at 0.55 $Å^{-1}$ becomes prominent even at the concentration <0.3 M (Section S4, Figure S13).[31] This ionic association is also seen from the relatively low ionic conductivity of concentrated TBA_3HCF solutions (see above). Our MD calculations (Figure S14) suggest that the correlation peak seen in SAXS corresponds to the average Fe−Fe distance of ∼11.3 Å between the HCF^{3-} anions contacting through an associated TBA^+ cation. The root cause for this strong ionic association is the relatively weak solvation of HCF^{3-} by MeCN molecules (see below). Consequently, despite the presence of 8−15 MeCN molecules in the solvation shell around HCF^{3-}, it is still strongly associated with the TBA^+ cations. That is, even the most polar aprotic solvent cannot fully screen the electrostatic attraction between the ions.

In general, the redox potential of a redoxmer is highly dependent on the solvation structure.[32,33] Unlike MeCN, water interacts strongly with HCF polyanion by forming multiple $CN^-\cdots H-O-H$ hydrogen bonds.[34] According to MD simulations, the composition of the solvation shell around HCF^{3-} undergoes dramatic changes when water is added (Figure 2a-c). Water molecules readily replace MeCN and TBA^+ even when its fraction is low (Figures 2b and S16−S17). As water content is increased, the average number of TBA^+ cations within 3 Å from the HCF^{3-} decreases from three to one, while the number of water molecules increases from 0 to 20, with the number of H-bonds per anion closely tracking this increase (Figure 2d). In concert, the mean distances to the TBA^+ and solvent molecules associated with the HCF^{3-} increase as the H-bonded water molecules screen their electrostatic interactions (Figure 2e). Importantly, most of these changes occur when the fraction of water is less than 20 mol % (8 vol %) as the H-bonding causes water molecules to become preferentially associated with the HCF polyanion. This tendency rationalizes Figure 1 as the redox potential near-perfectly tracks the compositional change in the solvation shell around the anion.

To characterize TBA_3HCF anolyte in nonaqueous electrolytes, it was initially tested in symmetric flow cells. These cells have been widely used to assess the chemical stability of redoxmers because redoxmer crossover is reduced in such cells.[35] The initial TBA_4HCF (the reduced form of TBA_3HCF) was prepared by electrochemical reduction of TBA_3HCF in a separate flow cell using synthetic tetrabutylammonium 2,2,6,6-tetramethylpiperidinyloxy-4-(3′-oxypropane-1′-sulfonate) as a catholyte material (TBA-SPrO-TEMPO, Scheme S1, Figures S4−S6 and S11). In this experiment, the cell was charged to 50% of the theoretical capacity (Figure S18). The obtained mixture containing 25 mM TBA_3HCF and 25 mM TBA_4HCF was placed into both compartments of a symmetric flow cell with a 175 μm Daramic porous membrane (Figure 3a, Section S6). The cell was cycled at a constant current density of 5 mA cm^{-2}. The completion of 1000 cycles took 425 h or 17.7 days. Figure 3b shows the Nuquist plots obtained before and after this cycling. The area-specific resistance (ASR) of 3.2 Ω cm^2 was obtained before cycling that increased slightly to 3.6 Ω cm^2 after cycling (Figure 3b). Figure 3c summarizes the cycling capacity, Coulombic efficiency (CE) and voltage profiles for this flow cell. The capacity decreased from 7.7 mAh (89% material utilization) to 6.3 mAh (73% utilization) over the first 200 cycles, followed by a slower decrease, which corresponds to the average capacity fade of 0.027% per cycle or 1.5% per day. Such a capacity profile is very similar to those for porous separator-based vanadium flow cells, and the ininitial capacity drop may be ascribed to a hydraulic pressure balancing process.[36,37] Nevertheless, this excellent capacity retention and the near-100% CE indicate high electrochemical stability of HCF. A stationary symmetric H-cell containing 5 mM HCF also exhibited negligible capacity fade over 180 cycles (32 h) with the CE approaching 100% (Section S6 and Figure S19). These stable cycling behaviors suggest the feasibility of

https://doi.org/10.1021/acsenergylett.4c01351
ACS Energy Lett. 2024, 9, 4273−4279

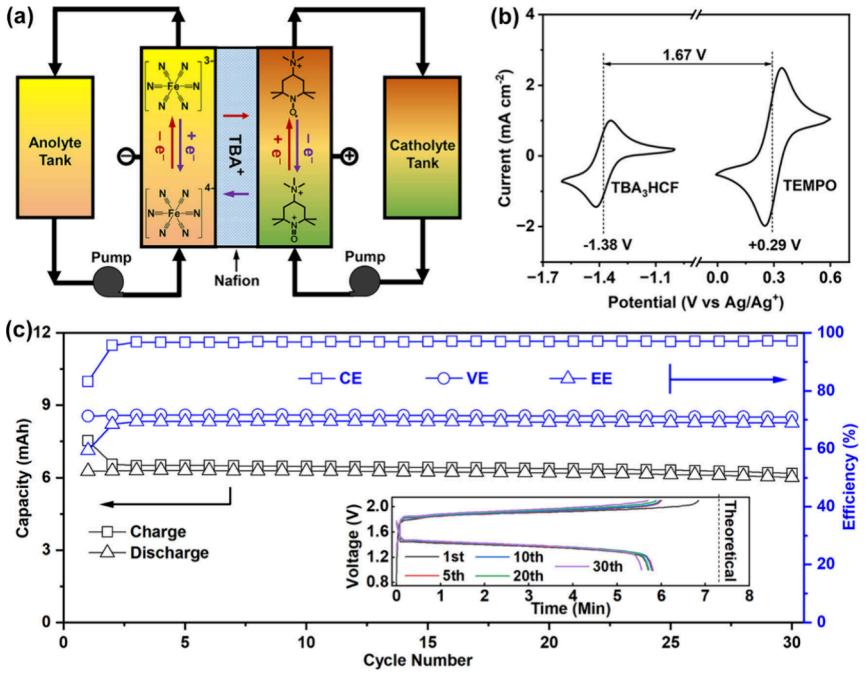

Figure 4. 50 mM TBA_3HCF/TEMPO flow cell with excess TEMPO: (a) schematic illustration; (b) CV curves of the two redoxmers at 10 mM concentration with a scan rate of 50 mV s^{-1}; (c) cyling capacities, efficiencies, and voltage curves (inset) of the flow cell at a current of 10 mA cm^{-2}.

transferring the stability advantage of HCF from aqueous to nonaqueous RFBs.

Encouraged by these results, we sought to demonstrate the use of TBA_3HCF as an anolyte candidate for full-cell nonaqueous RFBs by pairing it with TEMPO-based catholyte redoxmers (Section S7). In these experiments, TBA^+ exchanged Nafion cation exchange membranes were applied, expected to block the transport of polyanionic HCF across the membrane. Unfortunately, preventing crossover and parasitic reactions of the *catholyte* that we needed to pair with HCF *anolyte* proved to be an intractable challenge. When TBA-SPrO-TEMPO was used, rapid capacity fading was observed (Figure S20). According to the postcycling CV analysis, depletion of TBA-SPrO-TEMPO and formation of a new redox peak were observed in the corresponding compartment. When unmodified neutral TEMPO was used instead, the capacity retention was considerably improved but significant TEMPO crossover occurred (Figure S21). Despite the drawbacks of the selected catholyte, in all these full-cell tests, no chemical degradation or membrane crossover of HCF was detected by postcycling analysis. Thereby lies one of the key advantages, in terms of stability and impermeation, with the use of HCF polyanions in nonaqueous RFBs. The switch of electrolyte environment from aqueous to nonaqueous barely compromises the chemical stability of HCF, making it a highly adaptable redox candidate. The multiple negative charges in HCF electrostatically repulse it from the cation exchange membrane, which stands for a unique benefit over small organic redoxmers as for these molecules there are no good ways to suppress their membrane crossover. In addition, we have tried to slow down the crossover by using mixed-redoxmer electrolytes,[38,39] but the degradation of TEMPO was only accelerated (Figure S22).

To compensate for this degradation, we have cycled a flow cell containing 50 mM TBA_3HCF anolyte and excess 100 mM TEMPO catholyte, separated by a TBA^+-Nafion 115 membrane (Figures 4a and 4b). With an ASR of 29 Ω cm^2, the flow cell was cycled between 0.9 and 2.1 V at a constant current density of 10 mA cm^{-2}. Figure 4c shows the cycling performance of this cell over 30 cycles (5.5 h). The flow cell demonstrated the mean CE of 97%, the voltage efficiency (VE) of 71%, the energy efficiency (EE) of 69%, and the material utilization of ∼80%. The nearly flat capacity profile reiterates the previously demonstrated chemical stability and membrane impermeation of HCF. Once again, further cycling demonstrated rapid capacity fade due to fast TEMPO crossover but still with negligible CV impairment and membrane permeation for HCF anolyte (Figure S23). It is obvious that the catholyte becomes the limiting factor for long-cycling full-cell demonstration. Inspired by the HCF results, the molecular design approach of including the polyionic nature in a stable redox scaffold can be extended to the development of desired catholyte redoxmers although this is still quite challenging for high redox potential candidates. As our goal here is to establish the stability and blocking of HCF polyanion, the optimization of catholyte molecule for crossover is not in the scope of this study.

In this study, we demonstrate how a previously established aqueous catholyte can be re-enegineered into a novel anolyte for nonaqueous RFBs. To this end, the hexacyanoferrate(III) was paired with an organic cation to obtain an ionic compound with good solubility and ionic conductivity in MeCN. As MeCN around HCF polyanions replaces water molecules that are strongly H-bonded to cyano ligands, the redox potential decreases by more than 1 V. The resulting anolyte undergoes fully reversible one-electron redox reactions, which makes it competitive even with the best organic anolytes. Unlike the latter, HCF anolyte shows few if any parasitic reactions as suggested by our symmetric flow cell experiments. This exceptional stability in MeCN can be compared with the middling stability of HCF polyanions as a catholyte in aqueous RFBs. Our full cell experiments indicate that the polyanion is

https://doi.org/10.1021/acsenergylett.4c01351
ACS Energy Lett. 2024, 9, 4273−4279

fully blocked by Nafion cation exchange membranes; this blocking is difficult or impossible to achieve in nonaqueous RFBs with organic redoxmers.

To conclude, our study presents a new strategy for designing stable, impermeable redoxmers in nonaqueous RFBs. Large changes in redox potentials and wholly new properties can be obtained by transferring redox active polyvalent ions from aqueous to nonaqueous environments by pairing them with organic counterions. As blocking of such polyvalent ions using ion-exchange membranes is less challenging than blocking small organic molecules, this approach opens new possibilities in nonaqueous RFB design that have not been explored before.

■ ASSOCIATED CONTENT

Supporting Information

The Supporting Information is available free of charge at https://pubs.acs.org/doi/10.1021/acsenergylett.4c01351.

Sections S1 to S8 with narratives and figures detailing material synthesis, conductivity measurements, MD computations, CV testing, X-ray scattering, and flow cell tests (PDF)

■ AUTHOR INFORMATION

Corresponding Authors

Ilya A. Shkrob − *Joint Center for Energy Storage Research, Argonne National Laboratory, Lemont, Illinois 60439, United States; Chemical Sciences and Engineering Division, Argonne National Laboratory, Lemont, Illinois 60439, United States;* orcid.org/0000-0002-8851-8220; Email: shkrob@anl.gov

Xiaoliang Wei − *Department of Mechanical and Energy Engineering, Indiana University−Purdue University Indianapolis, Indianapolis, Indiana 46202, United States;* orcid.org/0000-0002-7692-2357; Email: xwei18@iupui.edu

Lu Zhang − *Joint Center for Energy Storage Research, Argonne National Laboratory, Lemont, Illinois 60439, United States; Chemical Sciences and Engineering Division, Argonne National Laboratory, Lemont, Illinois 60439, United States;* Email: zhanglu77@gmail.com

Authors

Yuyue Zhao − *Joint Center for Energy Storage Research, Argonne National Laboratory, Lemont, Illinois 60439, United States; Chemical Sciences and Engineering Division, Argonne National Laboratory, Lemont, Illinois 60439, United States; Department of Mechanical and Energy Engineering, Indiana University−Purdue University Indianapolis, Indianapolis, Indiana 46202, United States*

Sambasiva R. Bheemireddy − *Joint Center for Energy Storage Research, Argonne National Laboratory, Lemont, Illinois 60439, United States; Chemical Sciences and Engineering Division, Argonne National Laboratory, Lemont, Illinois 60439, United States*

Diqing Yue − *Department of Mechanical and Energy Engineering, Indiana University−Purdue University Indianapolis, Indianapolis, Indiana 46202, United States; School of Mechanical Engineering, Purdue University, West Lafayette, Indiana 47907, United States;* orcid.org/0000-0002-9162-9810

Zhou Yu − *Joint Center for Energy Storage Research, Argonne National Laboratory, Lemont, Illinois 60439, United States; Material Science Division, Argonne National Laboratory, Lemont, Illinois 60439, United States*

Mohammad Afsar Uddin − *Joint Center for Energy Storage Research, Argonne National Laboratory, Lemont, Illinois 60439, United States; School of Chemical Sciences and Beckman Institute for Advanced Science and Technology, University of Illinois at Urbana−Champaign, Urbana, Illinois 61801, United States; Instituto de Ciencia de Materiales de Madrid, Madrid 20849, Spain;* orcid.org/0000-0002-3217-5513

Haoyu Liu − *Chemical Sciences and Engineering Division, Argonne National Laboratory, Lemont, Illinois 60439, United States*

Zhiguang Li − *Joint Center for Energy Storage Research, Argonne National Laboratory, Lemont, Illinois 60439, United States; Chemical Sciences and Engineering Division, Argonne National Laboratory, Lemont, Illinois 60439, United States; Department of Mechanical and Energy Engineering, Indiana University−Purdue University Indianapolis, Indianapolis, Indiana 46202, United States; School of Mechanical Engineering, Purdue University, West Lafayette, Indiana 47907, United States*

Xiaoting Fang − *Chemical Sciences and Engineering Division, Argonne National Laboratory, Lemont, Illinois 60439, United States; Department of Mechanical and Energy Engineering, Indiana University−Purdue University Indianapolis, Indianapolis, Indiana 46202, United States; School of Mechanical Engineering, Purdue University, West Lafayette, Indiana 47907, United States*

Xingyi Lyu − *Department of Chemistry and Biochemistry, Northern Illinois University, DeKalb, Illinois 60115, United States;* orcid.org/0000-0002-5781-2486

Garvit Agarwal − *Joint Center for Energy Storage Research, Argonne National Laboratory, Lemont, Illinois 60439, United States; Material Science Division, Argonne National Laboratory, Lemont, Illinois 60439, United States;* orcid.org/0000-0002-7814-6072

Zhangxing Shi − *Chemical Sciences and Engineering Division, Argonne National Laboratory, Lemont, Illinois 60439, United States*

Lily A. Robertson − *Joint Center for Energy Storage Research, Argonne National Laboratory, Lemont, Illinois 60439, United States; Chemical Sciences and Engineering Division, Argonne National Laboratory, Lemont, Illinois 60439, United States;* orcid.org/0000-0002-8784-0568

Lei Cheng − *Joint Center for Energy Storage Research, Argonne National Laboratory, Lemont, Illinois 60439, United States; Material Science Division, Argonne National Laboratory, Lemont, Illinois 60439, United States;* orcid.org/0000-0002-3902-1680

Tao Li − *Joint Center for Energy Storage Research, Argonne National Laboratory, Lemont, Illinois 60439, United States; Department of Chemistry and Biochemistry, Northern Illinois University, DeKalb, Illinois 60115, United States; X-Ray Science Division, Argonne National Laboratory, Lemont, Illinois 60439, United States*

Rajeev S. Assary − *Joint Center for Energy Storage Research, Argonne National Laboratory, Lemont, Illinois 60439, United States; Material Science Division, Argonne National Laboratory, Lemont, Illinois 60439, United States;* orcid.org/0000-0002-9571-3307

Venkat Srinivasan − *Joint Center for Energy Storage Research, Argonne National Laboratory, Lemont, Illinois 60439,*

https://doi.org/10.1021/acsenergylett.4c01351
ACS Energy Lett. 2024, 9, 4273−4279

United States; Argonne Collaborative Center for Energy Storage Science, Argonne National Laboratory, Lemont, Illinois 60439, United States; orcid.org/0000-0002-1248-5952

Susan J. Babinec − *Argonne Collaborative Center for Energy Storage Science, Argonne National Laboratory, Lemont, Illinois 60439, United States;* orcid.org/0000-0002-9680-3160

Zhengcheng Zhang − *Joint Center for Energy Storage Research, Argonne National Laboratory, Lemont, Illinois 60439, United States; Chemical Sciences and Engineering Division, Argonne National Laboratory, Lemont, Illinois 60439, United States;* orcid.org/0000-0002-0467-5801

Jeffrey S. Moore − *Joint Center for Energy Storage Research, Argonne National Laboratory, Lemont, Illinois 60439, United States; School of Chemical Sciences and Beckman Institute for Advanced Science and Technology, University of Illinois at Urbana−Champaign, Urbana, Illinois 61801, United States;* orcid.org/0000-0001-5841-6269

Complete contact information is available at: https://pubs.acs.org/10.1021/acsenergylett.4c01351

Author Contributions

†Y.Z. and S.R.B. contributed equally.

Notes

The authors declare no competing financial interest.

■ ACKNOWLEDGMENTS

This work was financially supported by the National Science Foundation (Award No. CHE-2055222) and the Joint Center for Energy Storage Research (JCESR), an Energy Innovation Hub funded by the U.S. Department of Energy, Office of Science, and Basic Energy Sciences. This research was also supported by Laboratory Directed Research and Development (LDRD) funding from Argonne National Laboratory, provided by the Director, Office of Science, of the U.S. Department of Energy under Contract No. DE-AC02-06CH11357. We acknowledge a generous grant of computer time from the Argonne National Laboratory Computing Resource Center (Bebop). We also acknowledge the computational resources from Center for Nanoscale Materials, an Office of Science user facility, which was supported by the U.S. Department of Energy, Office of Science, Office of Basic Energy Sciences, under Contract No. DE-AC02-06CH11357. This research used resources of the Advanced Photon Source, a U.S. Department of Energy (DOE) Office of Science User Facility operated for the DOE Office of Science by Argonne National Laboratory under Contract No. DE-AC02-06CH11357. The submitted manuscript has been created by UChicago Argonne, LLC, Operator of Argonne National Laboratory ("Argonne"). Argonne, a U.S. Department of Energy Office of Science laboratory, is operated under Contract No. DE-AC02-06CH11357.

■ REFERENCES

(1) Weber, A. Z.; Mench, M. M.; Meyers, J. P.; Ross, P. N.; Gostick, J. T.; Liu, Q. Redox flow batteries: a review. *J. Appl. Electrochem.* **2011**, *41* (10), 1137−1164.

(2) Yang, Z.; Zhang, J.; Kintner-Meyer, M. C.; Lu, X.; Choi, D.; Lemmon, J. P.; Liu, J. Electrochemical energy storage for green grid. *Chem. Rev.* **2011**, *111* (5), 3577−3613.

(3) Singh, V.; Kim, S.; Kang, J.; Byon, H. R. Aqueous organic redox flow batteries. *Nano Research* **2019**, *12* (9), 1988−2001.

(4) Gong, K.; Fang, Q. R.; Gu, S.; Li, S. F. Y.; Yan, Y. S. Nonaqueous redox-flow batteries: organic solvents, supporting electrolytes, and redox pairs. *Energ Environ. Sci.* **2015**, *8* (12), 3515−3530.

(5) Li, M.; Rhodes, Z.; Cabrera-Pardo, J. R.; Minteer, S. D. Recent advancements in rational design of non-aqueous organic redox flow batteries. *Sustain Energ Fuels* **2020**, *4* (9), 4370−4389.

(6) Hogue, R. W.; Toghill, K. E. Metal coordination complexes in nonaqueous redox flow batteries. *Curr. Opin Electroche* **2019**, *18*, 37−45.

(7) Winsberg, J.; Hagemann, T.; Janoschka, T.; Hager, M. D.; Schubert, U. S. Redox-Flow Batteries: From Metals to Organic Redox-Active Materials. *Angew. Chem., Int. Ed. Engl.* **2017**, *56* (3), 686−711.

(8) Lai, Y. Y.; Li, X.; Zhu, Y. Polymeric Active Materials for Redox Flow Battery Application. *ACS Appl. Polym. Mater.* **2020**, *2* (2), 113−128.

(9) Liu, Y. H.; Goulet, M. A.; Tong, L. C.; Liu, Y. Z.; Ji, Y. L.; Wu, L.; Gordon, R. G.; Aziz, M. J.; Yang, Z. J.; Xu, T. W. A Long-Lifetime All-Organic Aqueous Flow Battery Utilizing TMAP-TEMPO Radical. *Chem-Us* **2019**, *5* (7), 1861−1870.

(10) Wei, X.; Xu, W.; Vijayakumar, M.; Cosimbescu, L.; Liu, T.; Sprenkle, V.; Wang, W. TEMPO-Based Catholyte for High-Energy Density Nonaqueous Redox Flow Batteries. *Adv. Mater.* **2014**, *26* (45), 7649−7653.

(11) Wei, X. L.; Cosimbescu, L.; Xu, W.; Hu, J. Z.; Vijayakumar, M.; Feng, J.; Hu, M. Y.; Deng, X. C.; Xiao, J.; Liu, J.; et al. Towards High-Performance Nonaqueous Redox Flow Electrolyte Via Ionic Modification of Active Species. *Adv. Energy Mater.* **2015**, *5* (1), 1400678.

(12) Hu, B.; DeBruler, C.; Rhodes, Z.; Liu, T. L. Long-Cycling Aqueous Organic Redox Flow Battery (AORFB) toward Sustainable and Safe Energy Storage. *J. Am. Chem. Soc.* **2017**, *139* (3), 1207−1214.

(13) Hu, B.; Liu, T. L. Two electron utilization of methyl viologen anolyte in nonaqueous organic redox flow battery. *J. Energy Chem.* **2018**, *27* (5), 1326−1332.

(14) Liu, T. B.; Wei, X. L.; Nie, Z. M.; Sprenkle, V.; Wang, W. A Total Organic Aqueous Redox Flow Battery Employing a Low Cost and Sustainable Methyl Viologen Anolyte and 4-HO-TEMPO Catholyte. *Adv. Energy Mater.* **2016**, *6* (3), 1501449.

(15) Hollas, A.; Wei, X. L.; Murugesan, V.; Nie, Z. M.; Li, B.; Reed, D.; Liu, J.; Sprenkle, V.; Wang, W. A biomimetic high-capacity phenazine-based anolyte for aqueous organic redox flow batteries. *Nature Energy* **2018**, *3* (6), 508−514.

(16) Romadina, E. I.; Komarov, D. S.; Stevenson, K. J.; Troshin, P. A. New phenazine based anolyte material for high voltage organic redox flow batteries. *Chem. Commun.* **2021**, *57* (24), 2986−2989.

(17) Chen, H. N.; Lu, Y. C. A High-Energy-Density Multiple Redox Semi-Solid-Liquid Flow Battery. *Adv. Energy Mater.* **2016**, *6* (8), 1502183.

(18) Fan, H.; Wu, W. D.; Ravivarma, M.; Li, H. B.; Hu, B.; Lei, J. F.; Feng, Y. Y.; Sun, X. H.; Song, J. X.; Liu, T. L. Mitigating Ring-Opening to Develop Stable TEMPO Catholytes for pH-Neutral All-organic Redox Flow Batteries. *Adv. Funct Mater.* **2022**, *32* (33), 2203032.

(19) Liu, B.; Tang, C. W.; Wei, W.; Zhang, C.; Jia, G. C.; Zhao, T. S. Developing terpyridine-based metal complexes for non-aqueous redox flow batteries. *Energy Storage Mater.* **2023**, *60*, 102808.

(20) Kwabi, D. G.; Ji, Y.; Aziz, M. J. Electrolyte lifetime in aqueous organic redox flow batteries: a critical review. *Chem. Rev.* **2020**, *120* (14), 6467−6489.

(21) Hu, M. W.; Wang, A. P.; Luo, J.; Wei, Q. H.; Liu, T. L. Cycling Performance and Mechanistic Insights of Ferricyanide Electrolytes in Alkaline Redox Flow Batteries. *Adv. Energy Mater.* **2023**, *13* (15), 03762.

(22) Fell, E. M.; De Porcellinis, D.; Jing, Y.; Gutierrez-Venegas, V.; George, T. Y.; Gordon, R. G.; Granados-Focil, S.; Aziz, M. J. Long-Term Stability of Ferri-/Ferrocyanide as an Electroactive Component

for Redox Flow Battery Applications: On the Origin of Apparent Capacity Fade. *J. Electrochem. Soc.* **2023**, *170* (7), 070525.
(23) Pahari, S. K.; Gokoglan, T. C.; Visayas, B. R. B.; Woehl, J.; Golen, J. A.; Howland, R.; Mayes, M. L.; Agar, E.; Cappillino, P. J. Designing high energy density flow batteries by tuning active-material thermodynamics. *Rsc Adv.* **2021**, *11* (10), 5432−5443.
(24) Wei, X. L.; Xu, W.; Huang, J. H.; Zhang, L.; Walter, E.; Lawrence, C.; Vijayakumar, M.; Henderson, W. A.; Liu, T. B.; Cosimbescu, L.; et al. Radical Compatibility with Nonaqueous Electrolytes and Its Impact on an All-Organic Redox Flow Battery. *Angew. Chem. Int. Edit* **2015**, *54* (30), 8684−8687.
(25) Gutmann, V.; Gritzner, G.; Danksagmüller, K. Solvent effects on the redox potential of hexacyanoferrate(III)-hexacyanoferrate(II). *Inorg. Chim. Acta* **1976**, *17*, 81−86.
(26) Noftle, R. E.; Pletcher, D. An Interpretation of the Formal Potential for the Ferricyanide Ferrocyanide Couple as a Function of Solvent Composition. *J. Electroanal. Chem.* **1990**, *293* (1−2), 273−277.
(27) Gritzner, G.; Danksagmüller, K.; Gutmann, V. Outer-sphere coordination effects on the redox behaviour of the $Fe(CN)_6^{3-}$Fe-$(CN)_6^{4-}$ couple in non-aqueous solvents. *Journal of Electroanalytical Chemistry and Interfacial Electrochemistry* **1976**, *72*, 177−185.
(28) Wei, X. L.; Pan, W. X.; Duan, W. T.; Hollas, A.; Yang, Z.; Li, B.; Nie, Z. M.; Liu, J.; Reed, D.; Wang, W.; Sprenkle, V. Materials and Systems for Organic Redox Flow Batteries: Status and Challenges. *ACS Energy Lett.* **2017**, *2* (9), 2187−2204.
(29) Cao, J. Y.; Tian, J. Y.; Xu, J.; Wang, Y. G. Organic Flow Batteries: Recent Progress and Perspectives. *Energ Fuel* **2020**, *34* (11), 13384−13411.
(30) Wang, H.; Sayed, S. Y.; Luber, E. J.; Olsen, B. C.; Shirurkar, S. M.; Venkatakrishnan, S.; Tefashe, U. M.; Farquhar, A. K.; Smotkin, E. S.; McCreery, R. L.; Buriak, J. M. Redox flow batteries: how to determine electrochemical kinetic parameters. *ACS Nano* **2020**, *14* (3), 2575−2584.
(31) Liu, X. Y.; Fang, L. Z.; Lyu, X.; Winans, R. E.; Li, T. Unveiling the Liquid Electrolyte Solvation Structure by Small Angle X-ray Scattering. *Chem. Mater.* **2023**, *35* (23), 9821−9832.
(32) Svith, H.; Jensen, H.; Almstedt, J.; Andersson, P.; Lundbäck, T.; Daasbjerg, K.; Jonsson, M. On the nature of solvent effects on redox properties. *J. Phys. Chem. A* **2004**, *108* (21), 4805−4811.
(33) Wang, H.; Emanuelsson, R.; Banerjee, A.; Ahuja, R.; Stromme, M.; Sjödin, M. Effect of Cycling Ion and Solvent on the Redox Chemistry of Substituted Quinones and Solvent-Induced Breakdown of the Correlation between Redox Potential and Electron-Withdrawing Power of Substituents. *J. Phys. Chem. C* **2020**, *124* (25), 13609−13617.
(34) Prampolini, G.; Yu, P.; Pizzanelli, S.; Cacelli, I.; Yang, F.; Zhao, J.; Wang, J. Structure and dynamics of ferrocyanide and ferricyanide anions in water and heavy water: An insight by MD simulations and 2D IR spectroscopy. *J. Phys. Chem. B* **2014**, *118* (51), 14899−14912.
(35) Milshtein, J. D.; Kaur, A. P.; Casselman, M. D.; Kowalski, J. A.; Modekrutti, S.; Zhang, P. L.; Attanayake, N. H.; Elliott, C. F.; Parkin, S. R.; Risko, C.; Brushett, F. R.; Odom, S. A.; et al. High current density, long duration cycling of soluble organic active species for non-aqueous redox flow batteries. *Energ Environ. Sci.* **2016**, *9* (11), 3531−3543.
(36) Wei, X. L.; Nie, Z. M.; Luo, Q. T.; Li, B.; Chen, B. W.; Simmons, K.; Sprenkle, V.; Wang, W. Nanoporous Polytetrafl uoroethylene/Silica Composite Separator as a High-Performance All-Vanadium Redox Flow Battery Membrane. *Adv. Energy Mater.* **2013**, *3* (9), 1215−1220.
(37) Li, B.; Luo, Q. T.; Wei, X. L.; Nie, Z. M.; Thomsen, E.; Chen, B. W.; Sprenkle, V.; Wang, W. Capacity Decay Mechanism of Microporous Separator-Based All-Vanadium Redox Flow Batteries and its Recovery. *ChemSusChem* **2014**, *7* (2), 577−584.
(38) Duan, W. T.; Huang, J. H.; Kowalski, J. A.; Shkrob, I. A.; Vijayakumar, M.; Walter, E.; Pan, B. F.; Yang, Z.; Milshtein, J. D.; Li, B.; et al. "Wine-Dark Sea" in an Organic Flow Battery: Storing Negative Charge in 2,1,3-Benzothiadiazole Radicals Leads to Improved Cyclability. *ACS Energy Lett.* **2017**, *2* (5), 1156−1161.
(39) Pahari, S. K.; Gokoglan, T. C.; Chaurasia, S.; Bolibok, J. N.; Golen, J. A.; Agar, E.; Cappillino, P. J. Toward High-Performance Nonaqueous Redox Flow Batteries through Electrolyte Design. *ACS Appl. Energ Mater.* **2023**, *6* (14), 7521−7534.

https://doi.org/10.1021/acsenergylett.4c01351
ACS Energy Lett. 2024, 9, 4273−4279